Journal of Dental Sciences (2018) 13, 334–341

Available online at www.sciencedirect.com

ScienceDirect

journal homepage: www.e-jds.com

Original Article

Acemannan increased bone surface, bone volume, and bone density in a calvarial defect model in skeletally-mature rats

Dyna Jeanne D. Godoy [a,b], Jaroenporn Chokboribal [c], Ruben Pauwels [d,e], Wijit Banlunara [f], Polkit Sangvanich [g], Sukanya Jaroenporn [h], Pasutha Thunyakitpisal [i*]

[a] *Dental Biomaterials Science Program, Graduate School, Chulalongkorn University, Bangkok, Thailand*
[b] *Department of Materials Science, Faculty of Science, Chulalongkorn University, Bangkok, Thailand*
[c] *Department of Materials Science, Faculty of Science and Technology, Phranakhon Rajabhat University, Bangkok, Thailand*
[d] *OMFS-IMPATH Research Group, Department of Imaging & Pathology, Biomedical Sciences Group, KU Leuven, Leuven, Belgium*
[e] *Department of Radiology, Faculty of Dentistry, Chulalongkorn University, Bangkok, Thailand*
[f] *Department of Pathology, Faculty of Veterinary Science, Chulalongkorn University, Bangkok, Thailand*
[g] *Department of Chemistry, Faculty of Science, Chulalongkorn University, Bangkok, Thailand*
[h] *Primate Research Unit, Department of Biology, Faculty of Science, Chulalongkorn University, Bangkok, Thailand*
[i] *Research Unit of Herbal Medicine, Biomaterial and Material for Dental Treatment, Department of Anatomy, Faculty of Dentistry, Chulalongkorn University, Bangkok, Thailand*

Received 7 February 2018; Final revision received 9 April 2018
Available online 20 July 2018

KEYWORDS
Acemannan;
Aloe vera;
Bone repair;
Microcomputed tomography;
Histopathology

Abstract *Background/purpose:* Acemannan, a β-(1–4)-acetylated polymannose extracted from *Aloe vera* gel, has been proposed as biomaterial for bone regeneration. The aim of this study was to investigate the effect of acemannan in calvarial defect healing.
Materials and methods: Acemannan was processed to freeze-dried sponge form and disinfected by UV irradiation. Thirty-five female Sprague–Dawley rats were used in the *in vivo* study. Seven-mm diameter mid-calvarial defects were created and randomly allocated into blood clot control (C), acemannan 1 mg (A1), 2 mg (A2), 4 mg (A4), and 8 mg (A8) groups (n = 7). After four weeks, the calvarial specimens were subjected to microcomputed tomography (microCT) and histopathological analysis.

* Corresponding author. Research Unit of Herbal Medicine, Biomaterial and Material for Dental Treatment, Department of Anatomy, Faculty of Dentistry, Chulalongkorn University, Bangkok 10330, Thailand. Fax: +662 2188899.
E-mail address: pthunyak@yahoo.com (P. Thunyakitpisal).

https://doi.org/10.1016/j.jds.2018.06.004

Results: MicroCT revealed a significant increase in bone surface and bone volume in the A1 and A2 groups, and tissue mineral density in the A4 and A8 groups compared with the control group ($p < 0.05$). Histologically, the acemannan-treated groups had denser bone matrix compared with the control group.
Conclusion: Acemannan is an effective bioactive agent for bone regeneration, enhancing bone growth as assayed in two- and three-dimensions.

Introduction

Materials promoting bone repair and regeneration are important in successfully treating bone defects. Factors such as aging and its associated diseases, altered bone homeostasis, and large defect size are burdens to patients' treatment in terms of cost, time, and quality of life. Currently, an autologous bone graft is considered the gold standard in bone repair and regeneration, possessing osteogenic, osteoinductive, and osteoconductive properties.[1] However, a second surgery that is associated with donor site morbidity is required to obtain the graft. Therefore, there are many studies being conducted to develop alternative materials that enhance bone repair and regeneration without this disadvantage.[2]

There has been a wide use of natural compounds since the growing acceptance of the role that they play in treatment and prevention of disease. Natural compounds have been considered as alternative or complementary tools to modern medicine that provides an efficacious option to a broader patient base.[3] In bone repair and regeneration, several natural polymers (e.g. proteins and polysaccharides) have demonstrated bioactivity and osteoconductivity.[4] Acemannan, β-(1—4)-acetylated polymannose, is a naturally-occurring polysaccharide and is the main active component of *Aloe vera* gel. In previous studies, acemannan enhanced oral aphthous ulcer healing, and induced reparative dentin and periodontium formation.[5–8] Acemannan has also been demonstrated to induce bone formation in extraction sockets.[9,10] To clarify and expand the application of acemannan in bone healing, more evidence must be gathered from different orthotopic sites using 3D measurement techniques that describe bone healing in quantity and quality. The calvarial defect is an excellent preclinical model widely-used to evaluate the biological, osteoconductive, and/or osteoinductive properties of biomaterials.[11] However, the action of acemannan in calvarial healing has not yet been reported. In the present study, the effect of acemannan on rat calvarial defect healing was investigated using microcomputed tomography (microCT) and descriptive histopathology. We hypothesized that acemannan would enhance bone regeneration in calvarial defects.

Materials and methods

Acemannan sponge preparation and characterization

Acemannan sponge preparation

Aloe barbadensis Miller (*A. vera*) was obtained from a supplier in Bangkok, Thailand and was identified by Assoc. Prof. Dr. Suchada Sookrong, Department of Pharmacognosy and Pharmaceutical, Faculty of Pharmaceutical Sciences, Chulalongkorn University, Thailand. Acemannan was extracted from fresh *A. vera* gel as previously described.[12] Briefly, homogenization, centrifugation, and alcohol precipitation of the *A. vera* leaf gel was performed to obtain opaque particles, which were lyophilized and subsequently pulverized.

The acemannan powder was further processed to freeze-dried sponges as previously described.[6] Briefly, acemannan was prepared in seven-mm diameter holders in 5% w/v of distilled water, and then freeze-dried. The acemannan sponges were generated respective of their treatment groups: 1 mg, 2 mg, 4 mg, and 8 mg. The sponges were UV irradiated for 1 h. The generated acemannan sponges were characterized before and after UV irradiation using ^{13}C-NMR, ^{1}H-NMR, FT-IR, and SEM.

Nuclear magnetic resonance (NMR) and Fourier transform infrared (FT-IR) spectroscopy

The structure and position of the acemannan functional groups were analyzed using ^{13}C-NMR, ^{1}H-NMR, and FT-IR as previously described.[12,13] For FT-IR analysis, the acemannan sponge was ground with 100 mg KBr. The IR spectra were recorded using an FT-IR spectrometer (Spectrum System 2000; PerkinElmer, Waltham MA, USA) at a wave number of 500—4000 cm^{-1} with 64 scans/spectrum.

Scanning electron microscopy (SEM)

The acemannan sponge was critical-point dried, sputter-coated with gold, and observed using an electron microscope (FEI Quanta, Netherlands). One hundred random pores were measured to determine the average pore diameter of the acemannan sponge before and after UV irradiation using the ImageJ software (NIH, USA).[14]

Animal surgery

A pilot study using the same methodology as the current study was conducted to determine the minimum number of rats required. The mean and standard deviation of bone volume (BV), a microCT parameter, was used to compute the required sample size using G*Power 3.1.9.2. At 80% power, a sample size of 30 rats was necessary to demonstrate significant differences between the groups. The sample size was adjusted to 35 considering the possibility of animal attrition.

The female Sprague—Dawley rats were obtained from the National Laboratory Animal Center, Mahidol University,

Nakon Pathom, Thailand. The rats were given access to water and food *ad libitum*, and maintained at 25 ± 1 °C with a 12 h light/12 h dark cycle during the course of the experiment. The protocol was approved by the Animal Ethics Committee, Faculty of Dentistry, Chulalongkorn University (Protocol Review No. 1232003). All procedures were carried out by the same investigator.

Craniotomies were performed when the rats were six months old. The animals were anesthetized intramuscularly with a mixture of 50 mg/kg ketamine HCl and 1 mg/kg xylazine HCl. A seven-mm diameter calvarial defect was generated using a trephine bur (Hu-Friedy, Chicago, IL, USA) in a central location between the two parietal bones across the midsagittal suture. The procedure was done under constant normal saline irrigation to avoid heat build-up at the surgical site.

The rats were randomly divided into five groups upon receipt of treatment (n = 7): acemannan sponge 1 mg (A1), 2 mg (A2), 4 mg (A4), and 8 mg (A8) groups. Some defects were left untreated to serve as blood clot control (C). After treatment, the periosteum and skin were sutured. The animals were observed until recovery before being returned to their cages. The exclusion criteria were: profuse bleeding during defect preparation, wound dehiscence > three-mm, or weight loss >10%. Body weights were recorded weekly.

The rats were sacrificed four weeks post-treatment. The calvarial specimens were obtained and fixed using methanol-free phosphate buffered formaldehyde for microCT and histopathological analysis.

MicroCT evaluation

The calvarial specimens were scanned using the μCT 35 imaging system (Scanco Medical, Brüttisellen, Switzerland). The samples were enclosed in 30-mm diameter cylindrical holders, with the coronal aspect of the calvaria in a horizontal position. Scanning was performed using the following parameters: 70 kVp x-ray tube potential, 800 ms integration time, 114 μA intensity, and 15 μm voxel size.

The samples were renamed by a third party before interpretation. All interpretations were done by the same investigator who was blinded to the sample treatment. Evaluation was done using Scanco Medical software version 6.0 (Scanco Medical, Brüttisellen, Switzerland). A cylindrical region of interest corresponding to the generated defect, seven-mm in diameter and covering the entire calvarial thickness, was selected for analysis. A constrained Gaussian filter with a sigma of 0.8 and a support of 1.0 was used to minimize image noise. Mineralized tissue was differentiated from non-mineralized tissue using the adaptive threshold command provided in the software. The calvarial specimens had an initial threshold of 175—215 per mille (1/1000). The following variables were measured: bone surface (BS, mm^2), bone volume (BV, mm^3), and tissue mineral density (TMD, mg HA/cm^3).

Histopathological analysis

After microCT evaluation, the fixed specimens were processed for histopathologic analysis. The specimens were decalcified in formic acid and sodium citrate buffer, dehydrated with ascending concentrations of alcohol, and cleared in xylene. The specimens were embedded in paraffin. Sections five-μm thick were obtained from the center of the defect perpendicular to the midsagittal suture. The sections were stained with hematoxylin and eosin, and the defect area was evaluated for cellular inflammatory cell infiltration, tissue response, and bone matrix organization.

Statistical analysis

The data were analyzed using SPSS version 17 (IBM, Chicago, IL, USA). The pore sizes of the acemannan sponge before and after UV irradiation were analyzed using the independent t test. One-way analysis of variance (ANOVA) and the Dunnett *post hoc* test were used to compare the microCT data between the treatment and the control groups. A p-value < 0.05 was considered significant.

Results

Acemannan sponge characterization

The ^{13}C-NMR, ^{1}H-NMR, FT-IR spectra, and SEM images of the acemannan sponge before and after UV exposure are shown in Fig. 1. Our data confirm that the polysaccharide extract in the freeze-dried sponges was acemannan. Furthermore, the peaks distinctive of acemannan were present in the spectra of the acemannan sponges before and after UV irradiation. In the SEM images, no signs of structural or surface deterioration were observed in the UV-treated acemannan sponges. The acemannan sponge had interconnected elliptical pores with an average pore size of 160.57 ± 11.21 and 158.07 ± 10.34 μm before and after UV irradiation, respectively. No significant difference in pore size was observed in the acemannan sponge before and after UV irradiation ($p > 0.05$).

Calvarial defect healing

All animals recovered uneventfully after surgery. The animals demonstrated a slow and steady increase in body weight. No significant differences in animal body weight were observed between the groups at any observation time point ($p > 0.05$) (data not shown).

Representative microCT images of the mean BV of the treatment groups are shown in Fig. 2. The region of interest was extended to include the defect borders. The 3D reconstructions revealed a formation pattern mostly extending from the defect border towards the center. Small islands of new bone were also present in center of defect. Increased bone formation was observed in the acemannan-treated groups compared with the control group. A significant increase in BS and BV were observed in the A1 and A2 groups compared with the control group, while A4 and A8 groups demonstrated significantly induced TMD compared with control group ($p < 0.05$; Fig. 3).

After four weeks, no trace of the acemannan sponge was observed in the defect area (Fig. 4). No inflammatory cell

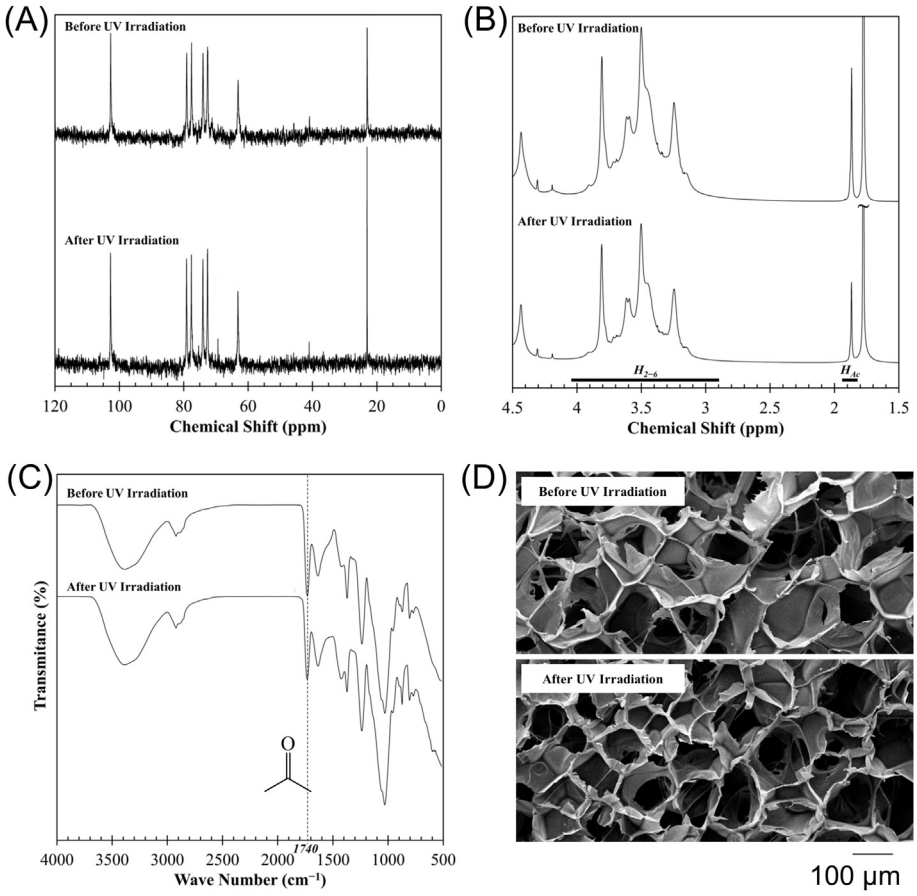

Figure 1 Acemannan sponge characterization before and after UV irradiation. The (A) ^{13}C-NMR, (B) ^{1}H-NMR, and (C) FT-IR spectra show that UV irradiation did not change the composition and molecular structure of acemannan. Furthermore, (D) SEM images show no sign of acemannan sponge deterioration after UV irradiation.

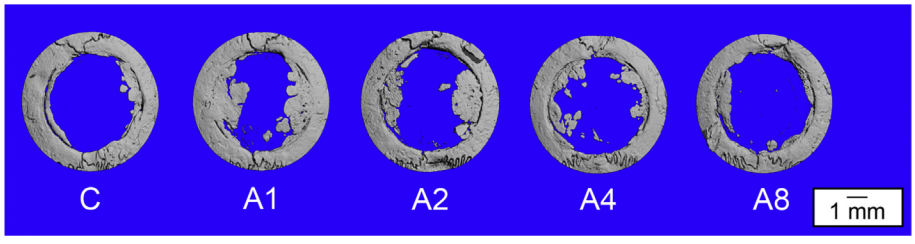

Figure 2 Representative 3D images of the experimental groups at four weeks post-treatment. Images shown are representative of the mean bone volume of each group. C: control; A1: acemannan 1 mg; A2: 2 mg; A4: 4 mg; and A8: 8 mg.

infiltration was observed in the acemannan-treated or blood clot control groups. The new bone formed was triangular in shape, with the vertex pointing inwards to the center of the defect. The representative histopathological images of the treatment groups are shown in Fig. 5. Cuboidal osteoblasts (arrowheads), were found lining areas of active bone formation around new bone. At the defect margin, there was direct contact between old bone and new bone (demarcated by arrows) in all groups. At higher magnification, the bone matrix of all acemannan-treated groups is denser than that of the control group.

Discussion

The present study investigated the effect of a range of acemannan concentrations on calvarial defect healing. Because of the biological inertness of the skull bones, calvarial defect healing takes place only when materials capable of promoting bone regeneration are applied.[15,16] To minimize the effect of increased bone regeneration due to physiological bone development, skeletally-mature rats were used in our study. According to Gasser and Willnecker,[17] female rats attain skeletal maturity at six months

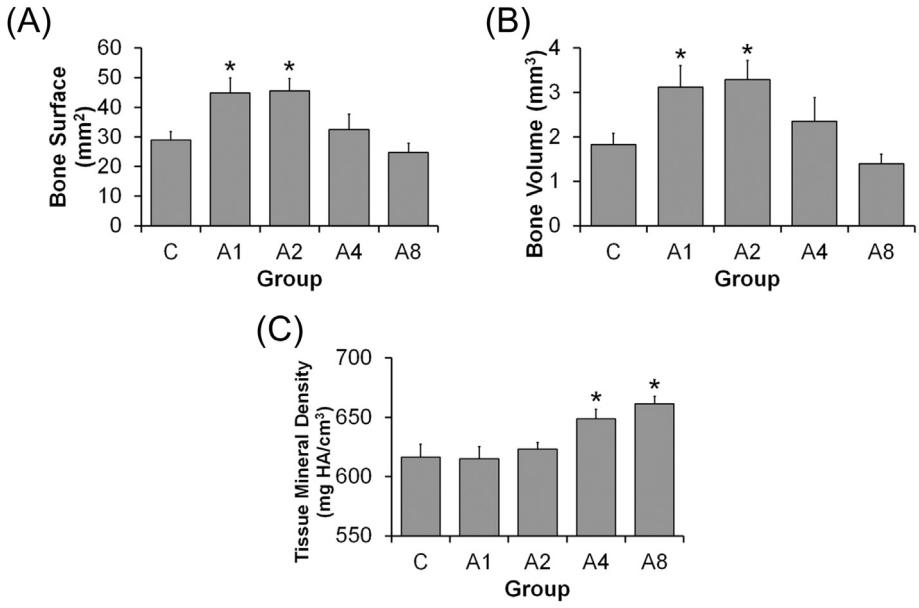

Figure 3 Acemannan stimulated bone healing in a calvarial defect model. Three bone morphometric parameters were measured: (A) bone surface, (B) bone volume, and (C) tissue mineral density. Asterisks indicate a significant difference compared with the blood clot control group (Mean $\pm$ SE, $p < 0.05$).

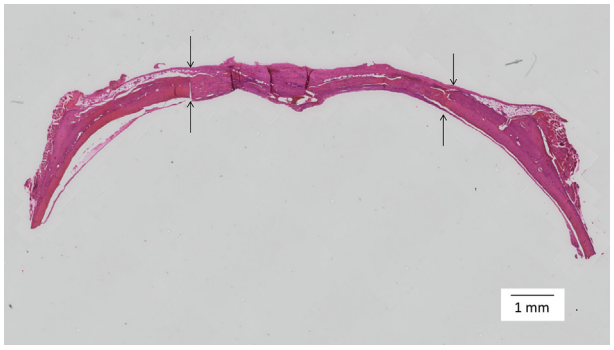

Figure 4 Photomicrograph of seven-mm diameter calvarial defect treated with acemannan sponge after four weeks. Arrows indicate the border of the defect.

old. Overall, our data revealed that acemannan stimulates bone growth compared with the control as assayed in two- and three-dimensions.

In this study, acemannan was applied to the calvarial defects in sponge form. As a sponge, acemannan was able to absorb and maintain interstitial fluid from the surrounding tissue to promote healing.[6] Furthermore, the sponges were disinfected using UV irradiation. Various methods have been suggested to treat biomaterials, including the use of sterilize grade filters, steam, or ethylene oxide.[18,19] However, these are not practical methods for acemannan sponge. This is because acemannan sponge would be unable to pass through a filter. Also, the steam sterilization technique (121 °C, 100 kPa for 15 min) would change the physical properties of the sponge, collapsing or dissolving it. Steam or autoclave sterilization is generally unsuitable for biomedical polymers and particular proteins. Significant changes in the molecular weight distribution and mechanical properties were observed after subjecting silk fibroin membranes to autoclave sterilization.[19] In another study, a biodegradable poly (caprolactone-urea) urethane membrane lost all structural morphology and integrity following autoclave sterilization.[20] In addition, during ethylene oxide sterilization, the toxic residual gas is entrapped in the surface or interconnected pores of the specimen and is released into the surrounding tissue. Several studies have shown the cytotoxic effects of bone replacement materials on fibroblasts and changes in cell morphology after ethylene oxide sterilization.[21–23] UV is a practical method used to disinfect acemannan sponge and is fast, low temperature, and leaves no toxic residues. Although UV has been reported to induce structural change at long exposure duration,[18] the NMR and FT-IR spectra of the acemannan sponge before and after UV irradiation indicated that 1 h exposure did not affect acemannan structure. Furthermore, cell migration and proliferation within UV-irradiated acemannan sponge has been previously demonstrated.[6]

Chantarawaratit et al. demonstrated that 10 mg acemannan induced new bone formation in a periodontal defect measuring around 40 mm^3.[6] Based on their results, we calculated that the effective dose of acemannan in our calvarial defect model is approximately 4 mg. Thus, 1, 2, 4, and 8 mg acemannan sponges were prepared and used in our study to determine the optimal concentration of acemannan to stimulate bone healing. In addition, 1 and 2 mg, and 4 and 8 mg acemannan concentrations differentially upregulated early and late osteoblast differentiation markers expression, respectively, *in vitro*.[9]

MicroCT is considered the gold standard in evaluating bone morphology and microarchitecture in small animal models, including rodents.[24] This technique allows direct 3D measurements without destroying the sample, and provides high-resolution data of bone quantity and structure. In our study, three variables were used to analyze new

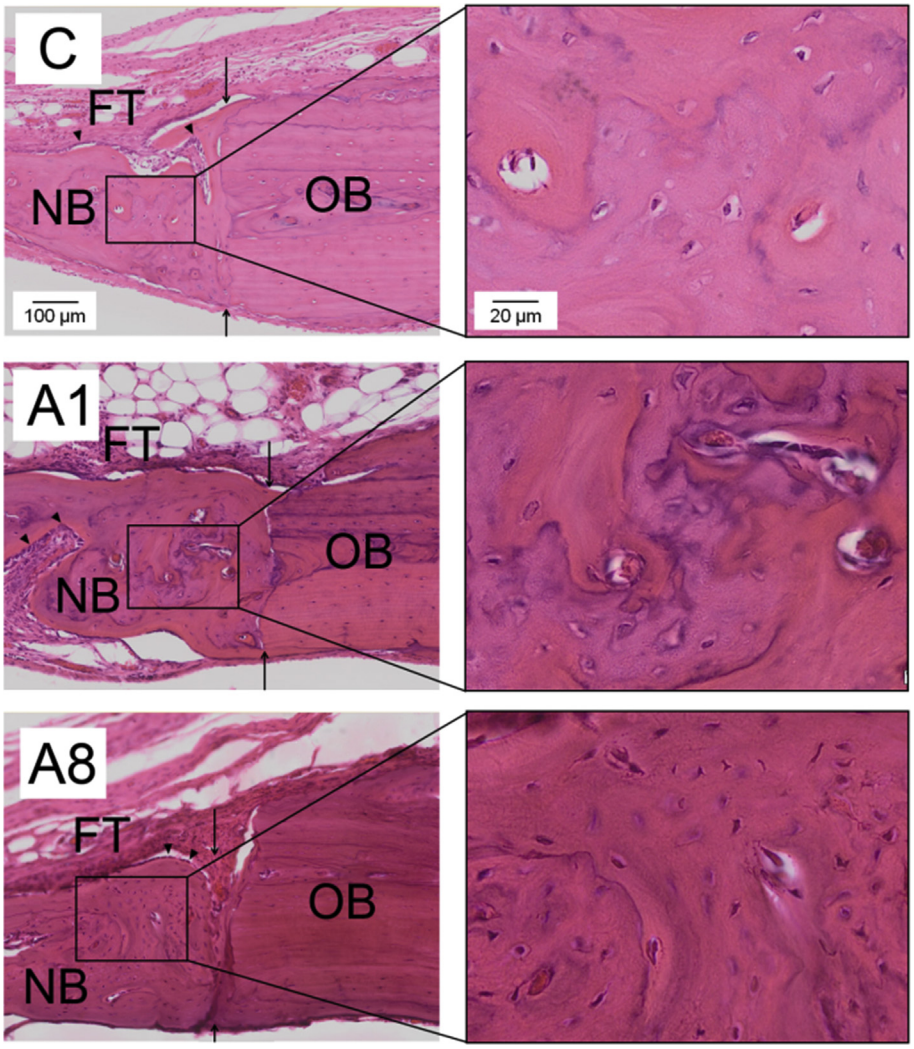

Figure 5 Representative histopathology of the experimental groups (C: control; A1: acemannan 1 mg; A8: acemannan 8 mg) four weeks post-treatment. Arrows indicate the defect border; Arrowheads indicate areas of active bone formation lined by cuboidal osteoblasts. The bone matrices are shown at higher magnification. OB-Old bone, NB-New bone, FT-Fibrous tissue. H&E stain.

bone quantitatively and qualitatively. BS, BV and TMD were used to represent the structural continuity, volume, and the degree of mineralization of new bone, respectively.[25,26] The significant increase in BS, BV, and TMD observed in this study indicate acemannan's ability to induce bone formation. From our results, 1 and 2 mg acemannan concentrations stimulated more bone growth, while 4 and 8 mg concentrations significantly improved the bone quality. Due to the limitations of the study methodology, an exact explanation of acemannan's dose-dependent effect on BS, BV, and TMD could not be stated. However, it is possible that this is due to a difference in bone healing stage induced by different concentrations of acemannan. The process of bone defect repair involves overlapping phases of inflammation, callus formation, and remodeling.[27] The early stages of repair is characterized by active bone formation, and results in a large woven bone callus. At later stages of bone repair, the woven bone remodels to a more compact lamellar structure similar to the mature bone. Thus, the decrease in BS and BV, and increase in TMD observed in the 4 and 8 mg acemannan groups might have resulted from the reduction in the bone callus size and change in structure as the bone remodels.[28] This indicates that the bone healing in the 4 and 8 mg acemannan groups is at a more advanced stage compared with the 1 and 2 mg groups. Further study could be conducted to confirm this hypothesis. The microCT findings were confirmed in the histopathology wherein the defects treated with acemannan presented a denser bone matrix compared with the control group. Furthermore, the absence of an inflammatory cell infiltrate, new bone growing from the defect margin, and good contact between the old bone and new bone demonstrate acemannan's wound healing promoting property,[29] biocompatibility, and ability to successfully integrate new bone with the old bone.

The findings in our study are consistent with previous reports indicating acemannan's osteoinductive effect. *In vitro*, acemannan enhanced the secretion of type I collagen and BMP-2, and the expression of osteoblast differentiation markers such as alkaline phosphatase, osteopontin, bone

sialophosphoprotein, and osteocalcin in bone marrow stem cells. *In vivo*, acemannan increased bone density in a rat tooth extraction socket model one month post-surgery.[9] Furthermore, radiographic evidence of increased bone density was observed three months post-surgery in a clinical study of extraction sockets treated with acemannan.[10]

The exact molecular mechanism by which acemannan affects cellular activity is not yet clear. However, it has been previously demonstrated that acemannan bioactivity can be partially-attributed to the free acetyl group in its mannose component.[13] Furthermore, acemannan upregulates TLR5/NF-κB dependent signaling pathway to activate its immunostimulatory effect in gingival fibroblasts.[30] In bone, NF-κB signaling plays a role in the proliferation and functions of osteoblasts and their precursors.[31] In conclusion, our data suggest that acemannan can be an effective bioactive agent for bone regeneration, enhancing bone surface, bone volume, and bone density in skeletally-mature rats.

Declarations of interest

The authors have no conflicts of interest relevant to this article.

Acknowledgments

We thank Prof. Suchinda Malaivijitnond, Prof. Dr. Visaka Limwong, Assoc. Prof. Dr. Dolly Methatharathip, and Dr. Kevin A. Tompkins for their valuable suggestions. This study was funded by Chulalongkorn University; Government Budget, Ratchadaphiseksomphot Endowment Fund Part of the "Strengthen CU's Researcher's Project", and The 90th Anniversary of Chulalongkorn University, Ratchadapiseksomphot Fund.

References

1. Schlundt C, Bucher CH, Tsitsilonis S, Schell H, Duda GN, Schmidt-Bleek K. Clinical and research approaches to treat non-union fracture. *Curr Osteoporos Rep* 2018;16:155–68.
2. Kolk A, Handschel J, Drescher W, et al. Current trends and future perspectives of bone substitute materials—From space holders to innovative biomaterials. *J Craniomaxillofac Surg* 2012;40:706–18.
3. Braithwaite MC, Tyagi C, Tomar LK, Kumar P, Choonara YE, Pillay V. Nutraceutical-based therapeutics and formulation strategies augmenting their efficiency to complement modern medicine: an overview. *J Funct Foods* 2014;6:82–99.
4. García-Gareta E, Coathup MJ, Blunn GW. Osteoinduction of bone grafting materials for bone repair and regeneration. *Bone* 2015;81:112–21.
5. Bhalang K, Thunyakitpisal P, Rungsirisatean N. Acemannan, a polysaccharide extracted from Aloe vera, is effective in the treatment of oral aphthous ulceration. *J Altern Compl Med* 2013;19:429–34.
6. Chantarawaratit P, Sangvanich P, Banlunara W, Soontornvipart K, Thunyakitpisal P. Acemannan sponges stimulate alveolar bone, cementum and periodontal ligament regeneration in a canine class II furcation defect model. *J Periodontal Res* 2014;49:164–78.
7. Jittapiromsak N, Sahawat D, Banlunara W, Sangvanich P, Thunyakitpisal P. Acemannan, an extracted product from Aloe vera, stimulates dental pulp cell proliferation, differentiation, mineralization, and dentin formation. *Tissue Eng Part A* 2010;16:1997–2006.
8. Songsiripradubboon S, Banlunara W, Sangvanich P, Trairatvorakul C, Thunyakitpisal P. Clinical, radiographic, and histologic analysis of the effects of acemannan used in direct pulp capping of human primary teeth: short-term outcomes. *Odontology* 2016;104:329–37.
9. Boonyagul S, Banlunara W, Sangvanich P, Thunyakitpisal P. Effect of acemannan, an extracted polysaccharide from Aloe vera, on BMSCs proliferation, differentiation, extracellular matrix synthesis, mineralization, and bone formation in a tooth extraction model. *Odontology* 2014;102:310–7.
10. Jansisyanont P, Tiyapongprapan S, Chuenchompoonut V, Sangvanich P, Thunyakitpisal P. The effect of acemannan sponges in post-extraction socket healing: a randomized trial. *J Oral Maxillofac Surg Med Pathol* 2016;28:105–10.
11. Vajgel A, Mardas N, Farias BC, Petrie A, Cimões R, Donos N. A systematic review on the critical size defect model. *Clin Oral Implants Res* 2014;25:879–93.
12. Jittapiromsak N, Jettanacheawchankit S, Lardungdee P, Sangvanich P, Thunyakitpisal P. Effect of acemannan on BMP-2 expression in primary pulpal fibroblasts and periodontal fibroblasts, in vitro study. *J Tissue Eng* 2007;4:149–54.
13. Chokboribal J, Tachaboonyakiat W, Sangvanich P, Ruangpornvisuti V, Jettanacheawchankit S, Thunyakitpisal P. Deacetylation affects the physical properties and bioactivity of acemannan, an extracted polysaccharide from Aloe vera. *Carbohydr Polym* 2015;133:556–66.
14. Schneider CA, Rasband WS, Eliceiri KW. NIH Image to ImageJ: 25 years of image analysis. *Nat Methods* 2012;9:671–5.
15. Bosch C, Melsen B, Vargervik K. Importance of the critical-size bone defect in testing bone-regenerating materials. *J Craniofac Surg* 1998;9:310–6.
16. Schmitz JP, Hollinger JO. The critical size defect as an experimental model for craniomandibulofacial nonunions. *Clin Orthop Relat Res* 1986;205:299–308.
17. Gasser JA, Willnecker J. Bone measurements by peripheral quantitative computed tomography in rodents. In: Helfrich MH, Ralston S, eds. *Bone research protocols*, 2nd ed. New Jersey: Humana Press, 2012:477–98.
18. Dai Z, Ronholm J, Tian Y, Sethi B, Cao X. Sterilization techniques for biodegradable scaffolds in tissue engineering applications. *J Tissue Eng* 2016;7. 2041731416648810.
19. Rnjak-Kovacina J, DesRochers T, Burke K, Kaplan D. The effect of sterilization on silk fibroin biomaterial properties. *Macromol Biosci* 2015;15:861–74.
20. Ahmed M, Punshon G, Darbyshire A, Seifalian AM. Effects of sterilization treatments on bulk and surface properties of nanocomposite biomaterials. *J Biomed Mater Res B Appl Biomater* 2013;101:1182–90.
21. Arizono T, Iwamoto Y, Okuyama K, Sugioka Y. Ethylene oxide sterilization of bone grafts: residual gas concentration and fibroblast toxicity. *Acta Orthop Scand* 1994;65:640–2.
22. Hastings C, Martin S, Heath J, Mark D, Mansfield J, Hollinger J. The effects of ethylene oxide sterilization on the in vitro cytotoxicity of a bone replacement material. *Toxicol In Vitro* 1990;4:757–62.
23. Kudryk VL, Scheidt MJ, McQuade MJ, Sutherland DE, Vandyke TE, Hollinger JO. Toxic effect of ethylene-oxide-sterilized freeze-dried bone allograft on human gingival fibroblasts. *J Biomed Mater Res* 1992;26:1477–88.
24. Bouxsein ML, Boyd SK, Christiansen BA, Guldberg RE, Jepsen KJ, Müller R. Guidelines for assessment of bone microstructure in rodents using micro–computed tomography. *J Bone Miner Res* 2010;25:1468–86.
25. Efeoglu C, Burke JL, Parsons AJ, et al. Analysis of calvarial bone defects in rats using microcomputed tomography:

potential for a novel composite material and a new quantitative measurement. *Br J Oral Maxillofac Surg* 2009;47:616—21.
26. Kazakia G, Burghardt A, Cheung S, Majumdar S. Assessment of bone tissue mineralization by conventional x-ray microcomputed tomography: comparison with synchrotron radiation microcomputed tomography and ash measurements. *Med Phys* 2008;35:3170—9.
27. Loi F, Córdova LA, Pajarinen J, Lin TH, Yao Z, Goodman SB. Inflammation, fracture and bone repair. *Bone* 2016;86:119—30.
28. Little D, Ramachandran M, Schindeler A. The anabolic and catabolic responses in bone repair. *J Bone Joint Surg Br* 2007; 89:425—33.
29. Choi S, Chung MH. A review on the relationship between Aloe vera components and their biologic effects. *Semin Integr Med* 2003;1:53—62.
30. Thunyakitpisal P, Ruangpornvisuti V, Kengkwasing P, Chokboribal J, Sangvanich P. Acemannan increases NF-κB/DNA binding and IL-6/-8 expression by selectively binding Toll-like receptor-5 in human gingival fibroblasts. *Carbohydr Polym* 2017;161:149—57.
31. Willett TL, Pasquale J, Grynpas MD. Collagen modifications in postmenopausal osteoporosis: advanced glycation endproducts may affect bone volume, structure and quality. *Curr Osteoporos Rep* 2014;12:329—37.